Published in final edited form as:
Biochim Biophys Acta. 2012 August ; 1823(8): 1273–1284. doi:10.1016/j.bbamcr.2012.05.012.

Mechanisms underlying the protein-kinase mediated regulation of the HERG potassium channel synthesis

Yamini Krishnan[a], **Yan Li**[a], **Renjian Zheng**[b,c], **Vikram Kanda**[b,c], and **Thomas V. McDonald**[a,b,c]

[b]Department of Medicine, Albert Einstein College of Medicine, Bronx, NY

[a]Department of Molecular Pharmacology, Albert Einstein College of Medicine, Bronx, NY

[c]Wilf family Cardiovascular Research Center, Albert Einstein College of Medicine, Bronx, NY

Abstract

The HERG (human *ether-a-go-go* related gene) potassium channel aids in repolarization of the cardiomyocyte membrane at the end of each action potential. We have previously shown that sustained protein kinase A or C (PKA and PKC) activity specifically enhances channel synthesis over the course of hours to days in heterologous expression and cardiac myocytes. The kinase-mediated augmentation of the channel is post-transcriptional and occurs near or at the endoplasmic reticulum. Here we report our further investigations into the mechanisms of kinase-mediated augmentation of HERG channel protein. We show that HERG channel phosphorylation alone is not sufficient for the PKA-dependent increase to occur. In vitro translation studies indicate that an additional factor is required for the process. Pharmacologic inhibitors suggest that the channel augmentation is not due to kinase-mediated alteration in proteasome or lysosome activity. PKA activation had no effect on stability of HERG mRNA and polyribosomal profiling showed that kinase activity did not elevate translation from low to high rates. Transcriptional inhibition results suggest that the additional cellular factor is a PKA-regulated protein. Together, these findings suggest that PKA-mediated augmentation of HERG abundance is more complex than previously appreciated involving enhancement of already active translation rates, phosphorylation of the channel protein and at least one other cAMP/PKA-responsive protein. Further exploration of molecular components of this regulatory pathway will be necessary to determine exact mechanism and the biomedical impact of this process in vivo.

Keywords

HERG; Protein kinase A; cyclic-AMP; protein translation; Protein kinase C; potassium channel

1. Introduction

The HERG (**h**uman ***e****ther-a-go-go* **r**elated **g**ene [1]) gene encodes the pore-forming α-subunit of the rapidly-activating delayed rectifier potassium channel I_{Kr} [2]. The HERG potassium channel function is essential for maintaining normal heart rate and rhythm in

Corresponding author: Thomas V. McDonald 1300, Morris Park Ave., Forchheimer G35, Bronx, NY 10461, USA Phone: +1 (718) 430-3370, Fax: +1 (718) 430-8989, tom.mcdonald@einstein.yu.edu.

humans. HERG channels are homo-tetrameric and carry the ventricular repolarization current I_{Kr} during phase three of the cardiac ventricular action potential. Mutations in the HERG gene are responsible for approximately 40% of all cases of the hereditary Long QT Syndrome (LQTS) [3]. LQTS may be a hereditary or an acquired cardiac disorder that predisposes patients to life threatening arrhythmias that can lead to syncope or sudden death. LQTS patients exhibit a prolonged interval between the beginning of the Q wave and the end of the T wave on body surface electrocardiograms. Hereditary HERG channel dysfunction occurs through deleterious mutations, whereas acquired LQTS can occur due to drug blockade of the channel pore or dysregulation of wild-type channels.

For patients with HERG mutations, cardiac events are often triggered by strong emotional or startling stimulus such as an alarm clock ringing and to a lesser extent with physical exertion [4]. Such triggers presumably increase the catecholamine concentration causing an acute rise in the adrenergic stimulation. In LQTS, electrical rhythm disturbances often degenerate into a dangerous form of polymorphic ventricular tachycardia called *Torsades des Pointes* [5]. An LQTS mutant HERG as in hereditary LQTS or a pharmacologically blocked HERG channel as in acquired LQTS would not respond appropriately in the setting of increased adrenergic stimulus and thus might lead to arrhythmia.

Previous work from several groups has shown that the K^+ current characteristics are acutely regulated by both α- and β-adrenergic stimulation [6–8]. Earlier studies showed that the acute effects of β-adrenergic signaling on HERG channel regulation are mediated directly via protein kinase A (PKA) phosphorylation of the channel and as well through direct binding of cAMP to the cyclic nucleotide binding domains on the channel [6]. A second level of β-AR/PKA regulation of HERG may occur with the association of adaptor proteins such as 14-3-3, which binds to HERG when the channel is phosphorylated and affects channel gating and duration of the response [9, 10]. Additionally, our group showed that an A-kinase anchoring protein (AKAP) is likely involved in targeting PKA to HERG in a macromolecular complex, which facilitates current modulation [11].

While the acute regulation has been well studied, the long-term adrenergic regulation of HERG is less clear. Our group has demonstrated that chronic β- and α-adrenergic stimulation distinctly enhances channel abundance over the time period of hours to days [12, 13]. The increase in HERG abundance did not appear to be at the level of transcription but did show accelerated channel synthesis. For the PKA mediated increase in HERG abundance, PKA activity must be localized to the surface of the ER [14]. We failed to observe similar kinase-mediated effects on other carfdac channels (KCNQ1, Kv1.5, Kir2.1) [12, 13]. Thus, we postulated that synthesis of the HERG channel is unusual in its responsiveness to the activity of kinases (PKA and PKC). Understanding which molecular components are involved and the signaling steps in this regulatory pathway is likely to reveal potential pharmacological targets for future therapies in acquired and hereditary forms of LQTS. In the present study, we sought to identify mechanisms responsible for the specific protein-kinase mediated increase in HERG protein abundance. We have determined: 1) that channel phosphorylation is necessary but not sufficient for the full increase to occur; 2) that a cellular co-factor is required for the kinase-induced increase in HERG channel abundance; 3) that changes in degradation pathways via the proteasome or lysosome do not account for the increase in HERG protein abundance; 4) that cAMP does not alter the stability of HERG mRNA significantly; 5) that there is not a measurable change in the association of HERG mRNA from low to highly translating ribosomes; and lastly 6) that the cellular co-factor is likely to be a cAMP/PKA-responsive protein.

2. Materials and Methods

2.1 Reagents

Unless otherwise noted, all chemicals were purchased from Sigma-Aldrich (St. Louis, MO) and Fisher Scientific (Waltham, MA). Small molecule activators and inhibitors were used at the following final concentrations: 50 μM 8-(4-chlorophenylthio)-adenosine-3',5'-cyclic monophosphate (CPT-cAMP), 10 μM H-89, 10 nM phorbol 12-myristate 13-acetate (PMA), 10 μM bisindolylmaleimide-1 (bis-1), 2 μM lactacystin, 750 μM MG132, 10 mM NH_4Cl, 50 nM concanamycin A, and 5 μg/ml actinomycin-D. Dimethylsulfoxide (DMSO) was used as the vehicle at a concentration of less than 0.1% in media. Antibodies against HERG were rabbit polyclonal H175, mouse monoclonal 9e10, and rabbit polyclonal A14 anti-myc antibodies (Santa Cruz Biotech, Santa Cruz, CA). Other antibodies used were pan-14-3-3 K-19 (Santa Cruz), PKA catalytic subunit–α (BD Biosciences, Franklin Lakes, NJ), PKA regulatory subunit RIIα (BD Biosciences), PKC isoform antibodies (BD Biosciences) and ubiquitin (Santa Cruz). Loading control antibodies used were against Na^+/K^+-ATPase (Thermo Fisher, Waltham, MA) and tubulin (Sigma).

2.2 Cell Culture, Transfection and Plasmids

For all experiments, HEK 293 (American Type Cell Culture, Manassas, VA) cells were maintained in RPMI1640 (Mediatech, Manassas, VA) supplemented with 10% fetal bovine serum (Hyclone/Thermo Fisher) and 10,000 IU of penicillin/streptomycin (Mediatech). Cells were kept at 37°C with humidified air and 5% CO_2. For some experiments culture dishes were coated with poly-L-lysine in 0.5% gelatin to help adherence.

Wild-type HERG was expressed with a C-terminal myc-tag in the pCI-neo mammalian expression vector as previously described [15]. The Δ1234-HERG is a mutated version in which the four PKA phosphate acceptor residues have been changed to alanine and preventing phosphorylation of the channel by PKA (S283A, S890A, T895A, and S1137A). Construction of this plasmid has been described earlier [6, 13]. The HERG-SD mutant contains four point mutations: S283D, S890D, T895D, and S1137D. This construct was created by sequential site directed mutagenesis of myc-tagged HERG in vector pCI-neo using the Quik-Change kit (Stratagene, Santa Clara, CA) (A more detailed description of the creation and characterization of the HERG-SD plasmid is given in the Supplemental Materials section). Mutations were confirmed by automated commercial sequencing (Genewiz Inc., South Plainfield, NJ). A second HERG construct was used where the HERG coding sequence was inserted as a restriction fragment (BanHI and HinDIII) into the multicloning site of pCMVtag3a vector (Stratagene) with an N-terminal myc-tag. This vector was used for in vitro translation experiments due to convenient restriction sites and RNA T3 polymerase site 5’ to the start codon. Moreover the N-terminal myc-tag allowed for immune-identification of all partially translated HERG products. 14-3-3ε was cloned into pcDNA3 vector (Invitrogen Life Sciences, Carlsbad, CA) at EcoRI and XhoI sites [9]. R56,60A 14-3-3η in pcDNA3.1 vector was a generous gift from Dr. Andrey Shaw (Washington University, St. Louis, MO). Difopein, a dimer of R18, a competitive binding inhibitor of all 14-3-3 isoforms [16], fused with c-Myc tag, was inserted into pEGFP-C1 vector (Clontech, Mountain View, CA).

Various constructs were expressed in HEK-HERG stable cells by transient transfection using LipofectAMINE 2000 (Invitrogen) in Opti-MEM medium (Gibco/Invitrogen). A total of 5 μg of DNA (pCDNA3-14-3-3ε, pcDNA3.1-R56,60A 14-3-3η (Δη), or pEGFP-Myc-Difopein) combined with 12 μL of LipofectAMINE 2000 diluted in 8 ml of Opti-MEM was used to transiently transfect one 100-mm dish with 80–90% confluence. Transfection medium was replaced by RPMI 1640 medium six hours later. Membrane permeable cAMP

analog CPT-cAMP (Sigma) was added to culture dish 10 hours after transfection. Cells were analyzed 48 hours after transfection. A green fluorescent protein (GFP) reporter plasmid (Clontech) was used to monitor transfection efficiency (at a molar ratio of 1:4 compared to that of the study plasmid). Stably transfected HEK-HERG and HEK-HERG-SD cells were created via limiting dilution cloning as previously described [11].

2.3 Western Blots and Immunoprecipitation

Forty-eight hours after transfection with the desired expression plasmids, HEK 293 cells were lysed with ice-cold NDET buffer (1% NP-40, 0.4% Deoxycholic acid, 5 mM EDTA, 25 mM Tris,150 mM NaCl, pH 7.5) with complete protease inhibitor cocktail (Roche, Indianapolis, IN) for 15 minutes. Cell lysates were centrifuged at 13,000 rpm at 4°C for 10 minutes to remove nuclei and insoluble debris, and the supernatants were mixed with SDS-PAGE loading buffer. Proteins were separated by 7.5% SDS-PAGE and transferred to nitrocellulose membranes (Bio-Rad, Hercules, CA) by semi-dry blotting unit (Fisher Biotech). The nitrocellulose membranes were blocked with Tris-buffered saline containing 0.5% Tween-20 (TBS-T) and 5% non-fat dry milk for 30 minutes at room temperature, and then incubated with primary antibody overnight at 4°C. The membrane was washed with TBS-T and then incubated in the corresponding infrared-fluorescence IRDye® 800 conjugated donkey anti-mouse and IRDye® 700DX conjugated donkey anti-rabbit secondary antibodies (1:10,000, Rockland Immunochemicals Inc., Gilbertsville, PA) for 30 minutes at room temperature in the dark followed by washing with TBS-T. The membranes were then scanned to visualize the signal at 680 nm or 780 nm by the Odyssey detection system (Li-Cor Biosciences, Lincoln, NE) and densitometry of the protein bands was performed using Li-Cor software.

For immuno-precipitation, the cells were lysed as above and the post-nuclear lysate was taken after a spin at 13,000 rpm at 4°C. A portion of the lysate was saved as input and the rest of the lysate was first pre-cleared for 30 minutes with non-specific IgG and then 30 minutes of protein A/G beads (Santa Cruz) at 4°C. The pre-cleared lysate was then immuno-precipitated for HERG using the myc-antibody overnight at 4°C. Fresh protein A/G beads were added and incubated for three hours at 4°C. The lysate was then spun, the supernatant was removed and beads were washed in NDET three times. A small volume of 4× SDS-PAGE loading buffer (Laemmli's buffer) was added to the beads and eluted for 30 minutes at room temperature. The samples were then separated on 4–15% gradient gels, transferred and blotted as described above.

2.4 In Vitro Translation

In vitro translation (IVT) experiments were done using the Promega micrococcal nuclease treated rabbit reticulocyte system and the protocol was adapted from Lu and Deutsch 2008 [17]. A plasmid containing the HERG coding sequence in pCMVtag3a were linearized using a restriction digest with MluI (New England Biolabs). Complementary RNA containing the 5' cap was transcribed in vitro from linearized plasmid DNA using the T3 Message Machine kit and purified on the MEGAClear column (Ambion/Life Sciences, Carlsbad, CA). The plasmid constructs (in pCMVtag3a) contained the HERG coding region but did not contain 5' or 3' untranslated regions. Proteins were synthesized in the presence of ^{35}S-methionine (EasyTag, Perkin Elmer, Waltham, MA) (1 μL per 25 μL reaction at a concentration of 10 μCi/μL) for 0 to 60 minutes at 30°C according to manufacturer's instructions. The small peptide inhibitor PKI 6-22 amide was added as indicated to a final concentration of 10 μM. For each sample 200 ng of cRNA was used for each 25-μL reaction. The reaction contained all essential reagents with canine pancreatic microsomal membranes and RNAsin RNAse inhibitor (Promega). Reactions were quenched on ice, in 4× volume of buffer composed of 20 mM HEPES, 4 mM $MgCl_2$, 100 mM NaCl, and 1 mM DTT, pH 7.4–7.5. The quenched

translation reactions were loaded onto a sucrose cushion of equal volume (containing 0.5 M sucrose, 100 mM KCl, 5 mM $MgCl_2$, 50 mM HEPES, 1 mM DTT, pH 7.5) and subjected to ultra-centrifugation using a TLA100.1 Beckman rotor at 77,000 rpm (200,000 × g) for 30 min at 4°C.The supernatant was removed and the pellet was resuspended in 10 μl of quench buffer and 10 μL SDS-PAGE sample buffer. Samples were loaded on to 4–15% gradient Tris-glycine gels and electrophoresed at constant voltage (Bio-Rad). Gels were then transferred using the semi-dry electro-blotting system onto nitrocellulose membranes. Membranes were then soaked in a solution of 0.5 M sodium salicylate, 5% methanol and 10% glycerol for 10 minutes and then exposed to film at 80°C for autoradiography.

2.4.1 IVT Analysis—Auto-radiography films were scanned and converted into digital files for densitometry analysis using ImageJ (National Institutes of Health) [18, 19]. Line scan analysis was done by taking a vertical line region of interest (ROI) for each lane. The values were then normalized from 0 to 1 and the highest peak, representing full-length product, was aligned.

For an additional quantitative measure 35S-methionine incorporation membranes were washed in Tris-buffered saline with Tween 20 (TBS-T) and then Ponceau S stained to visualize total protein and lane boundaries. Next, pieces were cut from each lane for liquid scintillation counting and quantitation. For HERG, a piece was cut between the molecular weight markers for 100 – 150 kD, representing full length product, and the rest of the lane representing the remainder was counted separately. Membrane pieces were dissolved in Filtron-X liquid scintillation cocktail (National Diagnostics, Atlanta, GA). The ratio of ^{35}S-methionine counts was calculated by taking the counts for full-length product divided by the counts of the remainder of the lane.

To determine the activity of PKA in the IVT system we used in vitro phosphorylation of the IVT lysate as previously published but with modifications [6]. In this case additional purified PKA catalytic subunit was either included or omitted but the IVT reaction lysate was complemented by 10 μM [γ-32P] ATP for 1 h at 30ºC. The reaction was terminated with ice-cold NDET buffer. The reaction mix was then subject to the centrifugation on sucrose cushion, as above, and separated on SDS-PAGE followed by autoradiography. Endogenous kinase was stimulated by cAMP and inhibited by staurosporine and the peptide PKI addition.

2.5 Polysomal Profiling

Linear 10–50% (w/v) sucrose gradients were prepared by consecutively freezing each layer until all five layers were added. Sucrose solutions of 10%, 20%, 30%, 40%, and 50% were made in the following buffer: 10 mM Tris pH 7.4, 100 mM NaCl, 2.5 mM $MgCl_2$ and RNAsin. For each Sw 41Ti tube, 2 mL of 50% sucrose was added to the bottom, frozen, the next 2 mL layer of 40% sucrose added, frozen, etc., until all five layers were added. Frozen gradients were thawed overnight at 4°C and ready to use the next day.

For polysomal profiling experiments, two 15 cm plates of stably transfected HEK-HERG cells (approximately 70% confluent) were used per gradient. Prior to lysis, cells were treated with 100 μg/mL cycloheximide for 10 minutes at 37°C. Dishes were placed on ice and cells were lysed on ice in a buffer composed of 100 mM NaCl, 2.5 mM $MgCl_2$, 25 mM, Tris-HCl pH 7.5, 1% NP-40, 0.4% sodium deoxycholate, 1mM DTT, 100 μg/ml cycloheximide, and RNAsin. The lysate was spun at 13,000 rpm on a table top centrifuge at 4°C for 10 minutes. A portion of the cleared lysate was saved for the total RNA measurement. The rest of the lysate (about 1–1.5 ml) was layered onto the top of the sucrose gradient. Gradients were spun at 38,000 rpm for 2 hours at 4°C using a Sw 41Ti rotor and Beckman Optima LE ultracentrifuge.

RNA was detected by measuring the absorbance at 254 nm using an ISCO UA-6 continuous UV reader. For each gradient, 1-mL fractions were collected into tubes containing 200 μl of 1% SDS. RNA was then extracted from the fractions by sodium acetate and ethanol precipitation with incubation at -80°C overnight. The samples were centrifuged at 13,000 rpm for 10 min at 4°C using a table-top centrifuge. The RNA pellets were re-suspended and purified using the RNEasy Mini Kit (Qiagen, Valencia, CA).

2.6 Quantitative Real-time PCR

First-strand synthesis was done on the pooled RNA gradient-fractions using the SuperScript VILO cDNA synthesis kit (Invitrogen). Groups of gradient-fractions were combined using equal volumes of RNA such that the total starting concentration for the first strand synthesis reactions was 2500 ng. The primers were a mix of oligo-dT and random hexamers. The reaction proceeded as follows using the Veriti thermo-cycler (Applied Biosystems, Carlsbad, CA): 10 min at 25°C, 50 min at 50°C, 5 min at 85°C and the final step included addition of *E.Coli* RNAse (Ambion) for 25 min at 37°C.

After first strand synthesis, qRT-PCR was done using Power SYBR green Master Mix and the Step One System (Applied Biosystems). Primers for HERG, GAPDH and β-actin were commercially synthesized (IDT DNA, Coralville IA). Reactions were prepared in triplicate. Cycling conditions were as follows: a holding stage 2 min at 50°C and 10 min at 95°C, 40 cycles of 15 sec 95°C, 1 min 60°C, 30 sec 72°C, and a final melt curve stage of 15 sec at 95°C, 1 min at 60°C, and 15 sec at 95°C.

Data were collected using the Step One Software to determine threshold-cycle (Ct) for relative quantification. Data analysis for polysome profiling was done by calculating the percent of total RNA for each fraction.

For experiments on total RNA samples (as in figure 4A), total HEK-HERG cellular RNA was obtained by lysis in NDET with RNAsin followed by a spin at 13,000 rpm to remove nuclei and debris. The cleared lysate was then purified using the RNEasy Mini kit as directed by manufacturer's instructions. The total RNA samples were quantified and then subjected to first strand synthesis and qRT-PCR as above. Analysis was done using the delta-delta Ct method and fold change in HERG mRNA was calculated using GAPDH as the control for normalization.

Primer Sequences: HERG forward: 5' TCAACCTGCGAGATACCAACATG 3' and reverse: 5'CTGGCTGCTCCGTGTCCTT 3'. GAPDH forward: 5' TCAACGACCACTTTGTCAAGCTCA 3' and reverse: 5' AGTAAGACCCCTGGACCACCAGC 3'. Actin forward: 5' CTCTTCCAGCCTT-CCTTCCT 3' and reverse: 5' CTGTACGCCAACACAGTGCT 3'.

2.7 Statistics

All data are expressed as the mean ± SEM. The two-tailed Student's T-test was used for pair-wise comparisons and a p-value of less than 0.05 was considered significant. For experiments comparing more than two means against the control condition, one-way ANOVA with Dunnett's test was used with p-value less than 0.05 considered significant.

3. Results

3.1 Phosphomimetic HERG mutant protein abundance also increases with kinase-stimulation

We have previously studied the effects of kinase stimulation by cAMP on HERG protein abundance and found that phosphorylation of HERG is likely involved [12, 13]. To further

characterize the participation of channel phosphorylation in cAMP/PKA enhancement of HERG abundance we compared wild type HERG (WT HERG); phospho-null mutant HERG (S283A, S890A, T895A, and S1137A known as Δ1234-HERG, which cannot be phosphorylated by PKA); and a phosphomimetic mutant HERG (HERG-SD) (Figure 1). In previous studies we showed that the Δ1234-HERG responded to PKA stimulation with minimal enhancement of channel protein [13]. We also created the PKA phosphomimetic mutant S283D, S890D, T895D, and S1137D (HERG-SD) where aspartic acid side chains resemble the chemical structure of a phosphorylated serine. HERG-SD appeared as a doublet on Western blot similar to wild type HERG (Figure 1A,C). In transient transfections using the same amount of initial plasmid DNA, the normalized expression level of HERG-SD on Western blot was 1.46±0.7 compared to HERG-WT at 1.0 however; this difference was not statistically significant (p-value = 0.5 and n=4). The morphology of HERG-SD currents and voltage dependence of activation were similar to wild type (Supplemental Figure 1). HEK cells stably expressing HERG-SD were created and then subjected to 24-hour kinase activation and/or inhibition. In side-by-side comparison wild type HERG showed a three-fold increase in protein abundance upon CPT-cAMP treatment and a six-fold increase upon PMA treatment (Figure 1A–B). For HERG-SD cAMP treatment resulted in a two-fold increase and PMA treatment resulted in a four-fold increase (Figure 1C-D). The inhibitor treatments mildly suppressed the abundance of wild type and HERG-SD. When CPT-cAMP stimulation of cells expressing Δ1234-HERG and WT HERG were compared, side-by-side, Δ1234-HERG showed a smaller degree of induction of channel protein (Fold-change = 1.64±0.125) compared to the increase in WT HERG (Fold-change = 3.97±0.355) (Figure 1E,F). This induction however was smaller than that seen for the HERG-SD mutant. Taken together, these findings suggest that channel phosphorylation is necessary but not sufficient to produce the entire increase in HERG abundance in response to kinase stimulation. One caveat however, is that aspartic acid substitution may not entirely mimic all properties of a phosphorylated serine (or threonine) and therefore the HERG-SD mutant may not behave exactly like a phosphorylated channel.

3.2 In-vitro translation (IVT) method reveals that a cellular co-factor is necessary for changes in HERG protein abundance

In our initial work we found that the cAMP/PKA-dependent increase in HERG was detectable as early as 60 minutes and metabolic labeling studies indicated that the increase was due to enhanced synthesis within 10–20 minutes [13]. In order to study the specific requirements for this enhanced synthesis regulation we sought to reconstitute the activity with the rabbit reticulocyte lysate (RRL). Such a reductionist method would allow us to precisely control those factors that might contribute to the regulation. The goal was to determine if activity of PKA alone could reproduce the increase in HERG protein abundance in the RRL in-vitro system. Upon initial assessment of the RRL components, we found that there was an easily detectable amount of PKA catalytic subunit already present in the system whereas PKC isoforms could not be detected (Figure 2A). Using purified complementary RNA of the full length HERG coding sequence in the translation reaction, we obtained a strong channel translation signal via incorporation of ^{35}S-Methionine (Figure 2B). The full length product is about 130 kD (indicated by arrow), which agrees with the expected size of non-glycosylated HERG [20]. The radio-labeled full-length and intermediate products were further identified as HERG by immunoblot analysis (Supplemental Figure 2). We next assayed for PKA-dependence in synthesis rates of HERG by perturbing PKA activity. When the PKA inhibitor, PKI 6-22 amide was included in the reaction we expected that the amount of HERG translation would decrease however, we found that there was no change in the amount of full-length protein produced or in the pattern of intermediate HERG products over the time course of 0 to 60 minutes (Figure 2B). Quantification of the ratio of final product over the total amount of intermediate products contained in the rest of the lane (a

measure of translation efficiency) showed no differences between the baseline and PKI treated condition at all time-points assayed (Figure 2C). Analysis of the pattern of intermediate products by line scans also showed no consistent differences in the amount or position of smaller molecular weight bands (Figure 2D). The line scan pattern of peaks was very reproducible between experiments. The peaks indicate accumulation of various intermediate length products where there may be slower or stalled translation, while the valleys would represent regions of the HERG peptide that are elongated rapidly enough as to prevent accumulation. Thus, the discrete peaks at ~40 and ~70 kD suggest areas of slowed translation elongation or stalled ribosomes. When PKA activity was enhanced in the IVT system by additional purified PKA catalytic subunit and ATP there was no significant change in the rate of HERG translation despite measurable kinase activity (Supplemental figures 2 and 3). Furthermore, we observed an IVT pattern similar to HERG with another cardiac K channel, KCNQ1—addition of exogenous PKA-catalytic subunit plus ATP failed to alter its translation rate (Supplemental figure 4). Thus, minimal cell-free translational machinery for HERG could not be regulated by PKA activity as occurs in intact cells. This indicates that 1) PKA activity is not required for the synthesis of HERG at baseline and 2) it also suggest that there may be a factor required for the increase in HERG synthesis that is present in HEK293 cells but is not present in the rabbit reticulocyte lysate system.

3.3 Proteasomal inhibition does not mimic the kinase-induced increase in HERG protein

Although our results were most consistent with cAMP/PKA enhancement of HERG abundance from accelerated synthesis awe sought to carefully examine possible contribution of channel degradation changes. We tested pharmacological inhibition of the proteasome and lysosome pathways separately. Figure 3 shows proteasome inhibition studies using lactacystin and MG132 in HEK-HERG cells stably expressing the channel. Lactacystin and MG132 are both cell permeable and specific inhibitors of proteasome subunits. Figure 3A and B show the effect of proteasome inhibition as compared to cAMP treatment. The immunoblot shows 24 hour treatment using the drugs alone or in combination. Proteasome inhibition did not significantly change the level of total HERG above control values. Furthermore, proteasome inhibition failed to significantly alter the PKA-dependent HERG augmentation. With proteasome inhibitor treatment there is less of the 155 kD form of HERG and this is a consistent finding among other groups [21, 22]. In figure 3C and 3D the same assay was repeated but used PMA treatment to stimulate PKC. As with cAMP/PKA stimulation, the changes in HERG abundance due to proteasome inhibition do not mimic the increased due to PKC activation, nor does proteasome inhibition significantly impact the kinase effect. As a positive control, we assayed total ubiquitin level as an indication of effective inhibition of the proteasome. Figure 3E and 3F show the proteasome inhibitors produced the expected increase in total ubiquitin, while kinase stimulation (via PKA or PKC) does not increase total ubiquitin-conjugated proteins. Furthermore, lysosomal inhibition was carried out using NH_4Cl and concanamycin A which are two methods that interfere with acidification of the lysosome, thereby reducing the proteolytic activity. After 24 hours of lysosomal inhibition no significant changes in HERG protein abundance was observed suggesting that kinase-mediated effects were unlikely due to reduction lysosomal degradation of the channel (Supplemental figure 4).

3.4 cAMP treatment does not alter HERG mRNA stability

Another possible mechanism for kinase augmentation of HERG that we considered was whether the stability of HERG mRNA was enhanced upon PKA stimulation. To test this we evaluated the mRNA abundance by quantitative RT-PCR after treatments with actinomycin-D (an inhibitor of new RNA transcription) over a time course after combination actinomycin-D and cAMP administration (Figure 4A). In the presence of actinomycin-D serial measurements of mRNA will reflect its rate of degradation within the cell. HEK-

HERG cells were treated with DMSO vehicle (control), 5 μg/ml actinomycin-D alone, or 5 μg/ml actinomycin-D together with 50 μM CPT-cAMP added simultaneously and cells were incubated for 6, 12, or 24 hours. The cells were then lysed in NDET with RNAse inhibitor and the cytoplasmic RNA was isolated via the RNEasy mini kit and analyzed through quantitative RT-PCR. We found that for both control and cAMP-stimulated cells actinomycin-D markedly reduced the HERG mRNA levels as expected. The combination actinomycin-D plus CPT-cAMP did not change the degree of HERG mRNA compared to actinomycin-D treatment alone at each of the three time points. This indicates that cAMP/PKA stimulation did not significantly alter the stability of HERG mRNA over 24-hours.

3.5 Polysomal profiling of HERG mRNA during kinase stimulation

Polysomal profiling is a method to determine relative distribution of an mRNA into pools with varying degrees of ribosomal occupancy that reflects translation activity. Changes in translation rates from low to high can be directly assayed by quantifying specific mRNAs among the polysomal profile. A redistribution of HERG mRNA from less-active polysome pools to more actively polysome pools during kinase activation would signify a direct enhancement in translation rate. We performed polysome profile analysis in HEK-HERG cells with quantitative real-time PCR (qRT-PCR) for baseline control and CPT-cAMP treatment conditions. Figure 4B–C shows polysome profiles for untreated and 6-hour treatment with CPT-cAMP. We chose this time point because previous studies indicated that changes in HERG protein abundance acceleration after kinase stimulation was most noticeable at 4–8 hours [13]. Figure 4B shows a polysome profile where the y-axis represents absorbance at 254 nm quantifying RNA concentration. The x-axis represents the direction of sedimentation where the highest density components are towards the right. The peaks of the profile from left to right represent the lightest components such as small soluble RNAs or mRNAs unassociated with ribosomes. The next large peak indicates the monosome fraction which mainly consists of mRNA occupied by a single ribosome. The monosome fraction is considered to represent least actively translated messages. The next group of peaks represents polysomes which are two or more ribosomes occupying an mRNA molecule which we separated into low molecular weight and high molecular weight polysomes (fractions 3 and 4). mRNAs that associate with polysomes are considered more actively translated. For qRT-PCR the polysome gradients were divided into four fractions (Figure 4C underlined segments). The shape and location of the peaks did not change significantly between untreated and treated conditions. A change in the ratio of peak heights would signal a global change in translation and this would presumably affect many cellular proteins. That the polysome profile shapes are not significantly changed upon kinase stimulation is consistent with our previous observation that cAMP-dependent increase of HERG protein was specific and did not alter other proteins we assayed [13],. The qRT-PCR analysis showed that HERG mRNA is highest in fraction 4 (high molecular-weight polysomes) in control samples which indicates that it is highly actively translated at baseline. The resolvable distribution of HERG mRNA showed no change with CPT-cAMP treatment (Figure 4D). The controls were GAPDH and actin which are both abundantly expressed in HEK cells (Figure 4E–F). Both GAPDH and actin are highest in fraction 4 and the distribution does not change significantly.

We previously showed that PKC activation also increased the abundance of HERG channel by a mechanism(s) that only partially overlap with those for PKA [12]. To investigate his we did polysomal profiling after PKC activation with PMA for 6-hours (Figure 5). The polysome profiles (Figure 5A–B) are similar in the height and shape of the peaks. The distribution of HERG mRNA is highest in fraction 4 and this does not change significantly with PKC activation (Figure 5C). Control mRNAs for GAPDH and Actin are not changed significantly with PMA treatment (Figure 5D–E). Taken together, the polysome profiling

data indicate that HERG mRNA is very actively translated at baseline and that kinase activation does not enhance channel abundance by raising the translation from low to high rates. The limitation of this assay however, resides in the inability to resolve among the higher density polysomes, particularly for long mRNAs such as HERG. Thus, the technique does not allow us to detect changes from high to very high levels of translation.

3.6 Transcriptional inhibition abrogates the cAMP-mediated HERG enhancement

Although kinase stimulation enhances HERG channel abundance in the absence of changes in HERG mRNA we sought to determine if new transcription of other intermediate protein co-factors were required for the effect. The fact that kinase-dependent regulation of translation could not be reconstituted in the cell-free IVT system suggested that such an additional cofactor was required. Figure 6A shows protein abundance for HERG and various other candidate co-factor proteins and compares cAMP treatment with transcriptional inhibition by actinomycin-D in stably expressing HEK-HERG cells. Cells were treated with DMSO vehicle (control), 5 μg/ml actinomycin-D alone, or 5 μg/ml actinomycin-D together with 50 μM CPT-cAMP added simultaneously and cells were incubated for 6, 12, or 24 hours. The cells were then lysed in NDET, and cytoplasmic lysates were assayed for HERG by Western blot. Over a time course of 6–24 hours, cAMP treatment resulted in a 1.5–2.5 fold increase in HERG protein abundance (Figure 6B). In the presence of actinomycin-D this effect was prevented. In light of the previous findings by Chen et al 2009 that the HERG mRNA remains stable and does not increase with 24 hours of kinase activation, our findings suggest that a short lived and/or newly transcribed protein is required for the PKA mediated increase in HERG protein abundance [13]. Three obvious candidate proteins are the PKA catalytic and regulatory subunits and the scaffolding/signaling protein 14-3-3 which interacts with HERG in a PKA-dependent fashion [9]. We immuno-blotted for these proteins and found no significant change in their abundances with the kinase stimulation, transcriptional inhibition or combination treatments. Thus, the protein co-factor(s) mediating kinase-enhancement of HERG synthesis remains unknown.

3.7 14-3-3 interactions do not alter the PKA mediated increase in HERG abundance

One potential role for 14-3-3 is to assist in trafficking of membrane proteins from the ER to the plasma membrane in a phosphorylation-dependent fashion [23]. Since 14-3-3 is known to interact with HERG upon phosphorylation [9], we hypothesized that 14-3-3 could be mediating the observed increase in HERG abundance. 14-3-3 has been shown to modulate trafficking and ER exit of a few other membrane proteins such as the nicotinic acetylcholine receptor (nAchR) and the KCNK3 potassium channel [24, 25]. To explore the participation of 14-3-3 in the CPT-cAMP stimulated increase in HERG, we used two different constructs to disrupt the interaction. The dominant-negative mutant 14-3-3Δ| R56,60A prevents 14-3-3 dimerization such that excess mutant protein will bind available sites on HERG but block dimerization of other 14-3-3 subunits [26]. We also used difopein—a dimer of the R18 peptide that is an effective tool to block 14-3-3 binding to any classical targets [16]. We compared the efficiency of these two methods (Figure 7A). Difopein (difo), 14-3-3Δη R56,60A (Δη), and additional wild-type 14-3-3εεwere transiently transfected into HEK-HERG cells. The HERG channel complex was isolated by immunoprecipitation using a HERG specific antibody. As shown in the lower panel of Figure 7A, co-immunoprecipitation of the endogenous 14-3-3 with HERG protein was increased in the presence of additional 14-3-3ε. Over-expression of 14-3-3Δη largely suppressed endogenous 14-3-3 binding in favor of the mutant and difopein completely blocked HERG/14-3-3 binding.

We next tested the effect of blocking the 14-3-3/HERG interaction on the cAMP-dependent augmentation of protein abundance (Figure 7B–C). The Western blot shows stably

expressing HEK-HERG cells with the various co-transfections: GFP, 14-3-3ε, 14-3-3Δη, difopein and 24-hour cAMP stimulation. The enhancement of HERG with cAMP treatment was preserved in all conditions tested (Figure 8C). This suggests that the PKA-mediated increase HERG abundance occurs independently of interactions with 14-3-3 proteins.

3.8 MiRP (KCNE) proteins in the cAMP/PKA augmentation of HERG

Another obvious family of HERG-interacting proteins to consider as playing a role in the kinase-mediated augmentation of channel translation is that encoded by the KCNE1 and KCNE2 genes—minK and MiRP1 [15, 43]. To examine the effects of KCNE subunit co-expression on the kinase-mediated enhancement of HERG we transiently co-transfected either KCNE1 (minK) or KCNE2 (MiRP1) with HERG in HEK cells and applied 50μM CPT-cAMP for 24-hours prior to immunoblot analysis (Figure 7D). Activation of cAMP/PKA increased the abundance of HERG signal in both groups to a comparable degree as in cells transfected with HERG alone with no statistically significant difference. Thus, minK and MiRP1 interaction with HERG are not mediators of regulators of the kinase-dependent enhancement of channel synthesis.

4. Discussion

In this work we have examined possible underlying mechanisms that could contribute to the specific, kinase-mediated increase in HERG protein abundance. We explored cellular aspects of PKA signaling that might contribute to changes in HERG protein abundance, we investigated changes in HERG translation rates and we examined potential involvement of altered channel degradation. We showed that the phospho-mimetic HERG mutant protein increases in abundance upon PKA or PKC stimulation, albeit to a lesser degree than wild type HERG. Given that the phospho-null mutant increased upon PKA activation even less than the phosphomimetic HERG [13], we posit that phosphorylation of HERG is necessary but not sufficient to produce the increase in protein abundance. The augmentation of the phospho-mimetic HERG-SD upon PKA stimulation strongly suggests the presence of additional PKA targets that necessary for the channel augmentation. Our finding that the in-vitro translation system was not able to recapitulate PKA-dependent enhancement of HERG further points to the existence of a cellular co-factor that is not present in the reticulocyte lysate system. Such a cofactor could be a small molecule messenger or protein whose expression or activity is induced by PKA—the latter is clearly possible since no de novo transcription of proteins occurs in the reticulocyte lysate system. That HERG translation in the cell-free system was unregulated by PKA activity perturbation also suggests that baseline translation does not absolutely require PKA activity.

Our investigations with transcriptional inhibition using actinomycin-D produced two important findings pertaining to kinase-regulated synthesis if HERG. First, we confirmed that kinase activation did not enhance the stability of HERG mRNA in actinomycin-D-chase experiments that abolished new transcription (Figure 5A). Second, inhibition of new transcription prevented the kinase enhancement of HERG abundance. In light of our previous finding that HERG mRNA levels remain unperturbed by 24 hours of cAMP treatment [13], our current results suggest that 1) increased levels of HERG mRNA are not responsible for the increase in HERG protein abundance and 2) that there is a PKA-responsive, short-lived or newly transcribed protein co-factor that is required for the regulatory process. These findings are consistent with the cell-free IVT results suggesting that a cellular co-factor is necessary for kinase-mediated augmentation of HERG channel abundance. Some initial candidate proteins we considered were PKA catalytic and regulatory subunits, 14-3-3 however; kinase activation did not affect the abundance of these proteins

The evidence from the present study and our prior work points towards accelerated translation of the HERG message. In an attempt to gain further insight into this process we utilized polysomal profiling as a measure of rates of specific mRNA translation. These experiments showed us that HERG is translated at a high level at baseline and that this is not detectably accelerated by PKA or PKC activation. There are several limitations to this analysis however, that need to be considered when interpreting. The HERG mRNA is a large message (3480bp for coding region alone), thus we expect it to sediment in a relatively heavy polysome fraction even if it were sub-maximally translated compared to smaller proteins for which this analysis has been used. Furthermore, there is an inherent limitation of the resolution in the high molecular weight/density range using sucrose gradients that precludes the ability to distinguish quantitative differences in this range. Thus, it is likely that HERG translation rates may increase within a moderate to high range that is not resolvable by the technique.

Emerging theories support a role for regulation of translation efficiency as a major contributor to protein abundance [27, 28]. Just how PKA activation enhances an already actively translating HERG channel is yet to be precisely determined. Our interpretation of the results favors the existence of a PKA-responsive protein co-factor(s) that in combination with direct phosphorylation of the channel upregulate synthesis of HERG. To date, the identity of such co-factors remains elusive. One large class of proteins to consider would be chaperones. In our previous study, we found that geldanamycin, an Hsp90 inhibitor, abolished the kinase-dependent increase in HERG abundance. It is plausible that a chaperone is specifically required for HERG synthesis and that this chaperone/co-factor has a short life cycle (Figure 8). It could be rapidly transcribed in response to increased cAMP or an increase in HERG synthesis and then subsequently degraded. Several candidate chaperones such as Hsp90, Hsc/Hsp 70, FKBP38 and Hsp40 have been identified in proteomics screens to interact with HERG [22, 29, 30]. Further investigation is necessary to determine each of the chaperones that interact with HERG and if the chaperone-HERG interactions are regulated by increased cAMP or PKA activation.

It is possible that specific aspects of HERG mRNA secondary structure or codon usage may affect translation and be regulated by PKA signaling. The secondary structure of mRNA is known to affect many aspects of translation such as recruitment of initiation factors and the initiation process itself [31]. There are also new theories about hierarchical recruitment of some mRNAs to the ER-associated ribosomes in order to translate proteins and how this is regulated [32]. An interesting avenue of further exploration would be to determine the spatial distribution of ribosomes on the HERG mRNA (ribosome density) and if this pattern could be regulated in a PKA-dependent manner [33, 34].

Another factor to consider is the folding of nascent HERG channels. Many proteins achieve their native conformations co-translationally and this is an important point of regulation. An interesting review notes that the coiled-coil motif in certain proteins can be regulated by phosphorylation and as an example a study by Szilak et al showed that the bZIP protein had increased stabilized and enhanced functionality by PKA-mediated phosphorylation of its coiled coil motif [35, 36]. HERG is thought to contain a tetramerization coiled coil domain in its distal C-terminus, which is in the vicinity of the fourth PKA consensus site, and this could possibly be a site for regulation [37].

Many studies have shown HERG is a protein that is prone to misfolding and increased degradation by the proteasome [21, 38, 39]. Several LQT2 mutants are also known to be degraded via ER-associated degradation (ERAD) and the ubiquitin-proteasome pathway, so we sought to determine whether proteasomal inhibition was a point of regulation which could be responsible for the increase in protein abundance. We found that pharmacological

proteasome inhibition changed HERG abundance modestly but did not cause a significant fold-change compared to kinase activation. We also considered recycling of HERG and through 24-hour lysosomal pharmacological inhibition, we determined that the changes in HERG protein abundance were minor, and could not account for the 2–4 fold increase observed with kinase activation. HERG has been shown to take an atypical route to the plasma membrane possibly involving an endosomal compartment as well as regulation at the ER-Golgi intermediate compartment [40, 41]. It is possible that a portion of HERG resides in these alternative compartments may not be amenable to the pharmacological inhibition techniques that we used. Considering that HERG has a long half-life (~12 hours) and that our previous data showed an increase in protein abundance as early as 4 hours with a maximal fold change of 4–5 fold at 24 hours, it appears unlikely that a change in degradation could account for the majority of the increase we observe. Another degradation pathway that we did not directly investigate is the upstream signaling of the unfolded protein response (UPR). One study showed that heterologous over-expression of an LQT2 mutant activated the UPR pathway [42]. It is conceivable that a baseline level of UPR response controls wild type HERG protein abundance and that activation of PKA-mediated pathway inhibits the baseline amount of degradation.

A potential limitation of our study is that the experiments were carried out in a heterologous over-expression cell culture system which imposes a significantly different context than that of a cardiomyocyte. It is possible that the cardiomyocyte contains specific isoforms or different expression patterns of the possible key mediators we have discussed above. Nevertheless, we have shown that native ERG channel protein is upregulated in rabbit myocytes upon PKA or PKC stimulation and heterologously expressed HERG in rat neonatal myocytes is also upregulated with PKA stimulation [12–14]. Further investigation is warranted to understand how HERG synthesis or trafficking is truly regulated in the cardiomyocyte and how this changes upon adrenergic stimulation.

Supplementary Material

Refer to Web version on PubMed Central for supplementary material.

Acknowledgments

The authors would like to thank Drs. Charles Rubin, Umadas Maitra and John Warner of Albert Einstein College of Medicine for invaluable advice and help throughout this project. This work was supported by funding from the NHLBI (F30HL096279 to Y.K. and HL077929 to T.V.M.) and American Heart Association (11GRNT5480008 to T.V.M.).

ABBREVIATIONS

HERG	human ether-a-go-go-related gene
HEK	human embryonic kidney
PKA	protein kinase A
PKC	protein kinase C
PMA	phorbol 12-myristate 13-acetate
CPT-cAMP	chlorophenylthiol-cyclic-AMP
H89	N-[2-(4-bromocinnamylamino)ethyl]-5-isoquinoline
Bis-I	bisindolylmaleimide I

References

1. Warmke JW, Ganetzky B. A family of potassium channel genes related to eag in Drosophila and mammals. Proc Natl Acad Sci U S A. 1994; 91:3438–42. [PubMed: 8159766]
2. Sanguinetti MC, Jiang C, Curran ME, Keating MT. A mechanistic link between an inherited and an acquired cardiac arrhythmia: HERG encodes the IKr potassium channel. Cell. 1995; 81:299–307. [PubMed: 7736582]
3. Saenen JB, Vrints CJ. Molecular aspects of the congenital and acquired Long QT Syndrome: Clinical implications. J Mol Cell Cardiol. 2008; 44:633–646. [PubMed: 18336833]
4. Schwartz PJ, Priori SG, Spazzolini C, Moss AJ, Vincent GM, Napolitano C, Denjoy I, Guicheney P, Breithardt G, Keating MT, Towbin JA, Beggs AH, Brink P, Wilde AA, Toivonen L, Zareba W, Robinson JL, Timothy KW, Corfield V, Wattanasirichaigoon D, Corbett C, Haverkamp W, Schulze-Bahr E, Lehmann MH, Schwartz K, Coumel P, Bloise R. Genotype-phenotype correlation in the long-QT syndrome: gene-specific triggers for life-threatening arrhythmias. Circulation. 2001; 103:89–95. [PubMed: 11136691]
5. Viskin S. Long QT syndromes and torsade de pointes. Lancet. 1999; 354:1625–33. [PubMed: 10560690]
6. Cui J, Melman Y, Palma E, Fishman GI, McDonald TV. Cyclic AMP regulates the HERG K(+) channel by dual pathways. Curr Biol. 2000; 10:671–4. [PubMed: 10837251]
7. Bian J, Cui J, McDonald TV. HERG K(+) channel activity is regulated by changes in phosphatidyl inositol 4,5-bisphosphate. Circ Res. 2001; 89:1168–76. [PubMed: 11739282]
8. Thomas D, Kiehn J, Katus HA, Karle CA. Adrenergic regulation of the rapid component of the cardiac delayed rectifier potassium current, I(Kr), and the underlying hERG ion channel. Basic Res Cardiol. 2004; 99:279–87. [PubMed: 15221346]
9. Kagan A, Melman YF, Krumerman A, McDonald TV. 14-3-3 amplifies and prolongs adrenergic stimulation of HERG K+ channel activity. EMBO J. 2002; 21:1889–98. [PubMed: 11953308]
10. Kagan A, McDonald TV. Dynamic control of hERG/I(Kr) by PKA-mediated interactions with 14-3-3. Novartis Found Symp. 2005; 266:75–89. discussion 89–99. [PubMed: 16050263]
11. Li Y, Sroubek J, Krishnan Y, McDonald TV. A-kinase anchoring protein targeting of protein kinase A and regulation of HERG channels. J Membr Biol. 2008; 223:107–16. [PubMed: 18679741]
12. Chen J, Chen K, Sroubek J, Wu ZY, Thomas D, Bian JS, McDonald TV. Post-transcriptional control of human ether-a-go-go-related gene potassium channel protein by alpha-adrenergic receptor stimulation. Mol Pharmacol. 2010; 78:186–97. [PubMed: 20463060]
13. Chen J, Sroubek J, Krishnan Y, Li Y, Bian J, McDonald TV. PKA phosphorylation of HERG protein regulates the rate of channel synthesis. Am J Physiol Heart Circ Physiol. 2009; 296:H1244–54. [PubMed: 19234087]
14. Sroubek J, McDonald TV. Protein kinase A activity at the endoplasmic reticulum surface is responsible for augmentation of human ether-a-go-go-related gene product (HERG). J Biol Chem. 2011; 286:21927–36. [PubMed: 21536683]
15. McDonald TV, Yu Z, Ming Z, Palma E, Meyers MB, Wang KW, Goldstein SA, Fishman GI. A minK-HERG complex regulates the cardiac potassium current I(Kr). Nature. 1997; 388:289–92. [PubMed: 9230439]
16. Masters SC, Fu H. 14-3-3 proteins mediate an essential anti-apoptotic signal. J Biol Chem. 2001; 276:45193–200. [PubMed: 11577088]
17. Lu J, Deutsch C. Electrostatics in the ribosomal tunnel modulate chain elongation rates. J Mol Biol. 2008; 384:73–86. [PubMed: 18822297]
18. Rasband, WS. ImageJ. U.S. National Institutes of Health; Bethesda, Maryland, USA: p. 1997-2011.http://imagej.nih.gov/ij
19. Abramoff MD, Magelhaes PJ, Ram SJ. Image Processing with ImageJ. Biophotonics International. 2004; 11:36–42.
20. Gong Q, Anderson CL, January CT, Zhou Z. Role of glycosylation in cell surface expression and stability of HERG potassium channels. Am J Physiol Heart Circ Physiol. 2002; 283:H77–84. [PubMed: 12063277]

21. Gong Q, Keeney DR, Molinari M, Zhou Z. Degradation of trafficking-defective long QT syndrome type II mutant channels by the ubiquitin-proteasome pathway. J Biol Chem. 2005; 280:19419–25. [PubMed: 15760896]
22. Walker VE, Wong MJ, Atanasiu R, Hantouche C, Young JC, Shrier A. Hsp40 chaperones promote degradation of the HERG potassium channel. J Biol Chem. 2010; 285:3319–29. [PubMed: 19940115]
23. Michelsen K, Yuan H, Schwappach B. Hide and run. Arginine-based endoplasmic-reticulum-sorting motifs in the assembly of heteromultimeric membrane proteins. EMBO Rep. 2005; 6:717–22. [PubMed: 16065065]
24. Jeanclos EM, Lin L, Treuil MW, Rao J, DeCoster MA, Anand R. The chaperone protein 14-3-3eta interacts with the nicotinic acetylcholine receptor alpha 4 subunit. Evidence for a dynamic role in subunit stabilization. J Biol Chem. 2001; 276:28281–90. [PubMed: 11352901]
25. O'Kelly I, Butler MH, Zilberberg N, Goldstein SA. Forward transport. 14-3-3 binding overcomes retention in endoplasmic reticulum by dibasic signals. Cell. 2002; 111:577–88. [PubMed: 12437930]
26. Thorson JA, Yu LW, Hsu AL, Shih NY, Graves PR, Tanner JW, Allen PM, Piwnica-Worms H, Shaw AS. 14-3-3 proteins are required for maintenance of Raf-1 phosphorylation and kinase activity. Mol Cell Biol. 1998; 18:5229–38. [PubMed: 9710607]
27. Schwanhausser B, Busse D, Li N, Dittmar G, Schuchhardt J, Wolf J, Chen W, Selbach M. Global quantification of mammalian gene expression control. Nature. 2011; 473:337–42. [PubMed: 21593866]
28. Vogel C, de Abreu RS, Ko D, Le SY, Shapiro BA, Burns SC, Sandhu D, Boutz DR, Marcotte EM, Penalva LO. Sequence signatures and mRNA concentration can explain two-thirds of protein abundance variation in a human cell line. Mol Syst Biol. 2010; 6:400. [PubMed: 20739923]
29. Walker VE, Atanasiu R, Lam H, Shrier A. Co-chaperone FKBP38 promotes HERG trafficking. J Biol Chem. 2007; 282:23509–16. [PubMed: 17569659]
30. Ficker E, Dennis AT, Wang L, Brown AM. Role of the cytosolic chaperones Hsp70 and Hsp90 in maturation of the cardiac potassium channel HERG. Circ Res. 2003; 92:e87–100. [PubMed: 12775586]
31. Kaufman RJ. Regulation of mRNA translation by protein folding in the endoplasmic reticulum. Trends Biochem Sci. 2004; 29:152–8. [PubMed: 15003273]
32. Chen Q, Jagannathan S, Reid DW, Zheng T, Nicchitta CV. Heirarchical regulation of mRNA Partitioning Between the Cytoplasm and the Endoplasmic Reticulum of Mammalian Cells. Mol Biol Cell. 2011; 22:2646–2658. [PubMed: 21613539]
33. Arava Y, Boas FE, Brown PO, Herschlag D. Dissecting eukaryotic translation and its control by ribosome density mapping. Nucleic Acids Res. 2005; 33:2421–32. [PubMed: 15860778]
34. Ingolia NT, Ghaemmaghami S, Newman JR, Weissman JS. Genome-wide analysis in vivo of translation with nucleotide resolution using ribosome profiling. Science. 2009; 324:218–23. [PubMed: 19213877]
35. Szilak L, Moitra J, Vinson C. Design of a leucine zipper coiled coil stabilized 1.4 kcal mol-1 by phosphorylation of a serine in the e position. Protein Sci. 1997; 6:1273–83. [PubMed: 9194187]
36. Burkhard P, Stetefeld J, Strelkov SV. Coiled coils: a highly versatile protein folding motif. Trends Cell Biol. 2001; 11:82–8. [PubMed: 11166216]
37. Jenke M, Sanchez A, Monje F, Stuhmer W, Weseloh RM, Pardo LA. C-terminal domains implicated in the functional surface expression of potassium channels. EMBO J. 2003; 22:395–403. [PubMed: 12554641]
38. Kagan A, Yu Z, Fishman GI, McDonald TV. The dominant negative LQT2 mutation A561V reduces wild-type HERG expression. J Biol Chem. 2000; 275:11241–8. [PubMed: 10753933]
39. Anderson CL, Delisle BP, Anson BD, Kilby JA, Will ML, Tester DJ, Gong Q, Zhou Z, Ackerman MJ, January CT. Most LQT2 mutations reduce Kv11.1 (hERG) current by a class 2 (trafficking-deficient) mechanism. Circulation. 2006; 113:365–73. [PubMed: 16432067]
40. Delisle BP, Underkofler HA, Moungey BM, Slind JK, Kilby JA, Best JM, Foell JD, Balijepalli RC, Kamp TJ, January CT. Small GTPase determinants for the Golgi processing and

plasmalemmal expression of human ether-a-go-go related (hERG) K+ channels. J Biol Chem. 2009; 284:2844–53. [PubMed: 19029296]

41. Smith JL, McBride CM, Nataraj PS, Bartos DC, January CT, Delisle BP. Trafficking-deficient hERG K channels linked to long QT syndrome are regulated by a microtubule-dependent quality control compartment in the ER. Am J Physiol Cell Physiol. 2011; 301:C75–85. [PubMed: 21490315]
42. Keller SH, Platoshyn O, Yuan JX. Long QT syndrome-associated I593R mutation in HERG potassium channel activates ER stress pathways. Cell Biochem Biophys. 2005; 43:365–77. [PubMed: 16244363]
43. Abbott GW, Sesti F, Splawski I, Buck ME, Lehmann MH, Timothy KW, Keating MT, Goldstein SA. MiRP1 forms IKr potassium channels with HERG and is associated with cardiac arrhythmia. Cell. 1999; 97:175–187. [PubMed: 10219239]

Highlights

- HERG channel synthesis is increased by protein kinase A (PKA) activity
- Channel phosphorylation is necessary but not sufficient for increased protein abundance
- PKA enhancement of HERG requires an additional protein co-factor
- Kinase activity does not elevate HERG translation from low to high rates
- Increased HERG abundance does not result from proteasome or lysosome inhibition

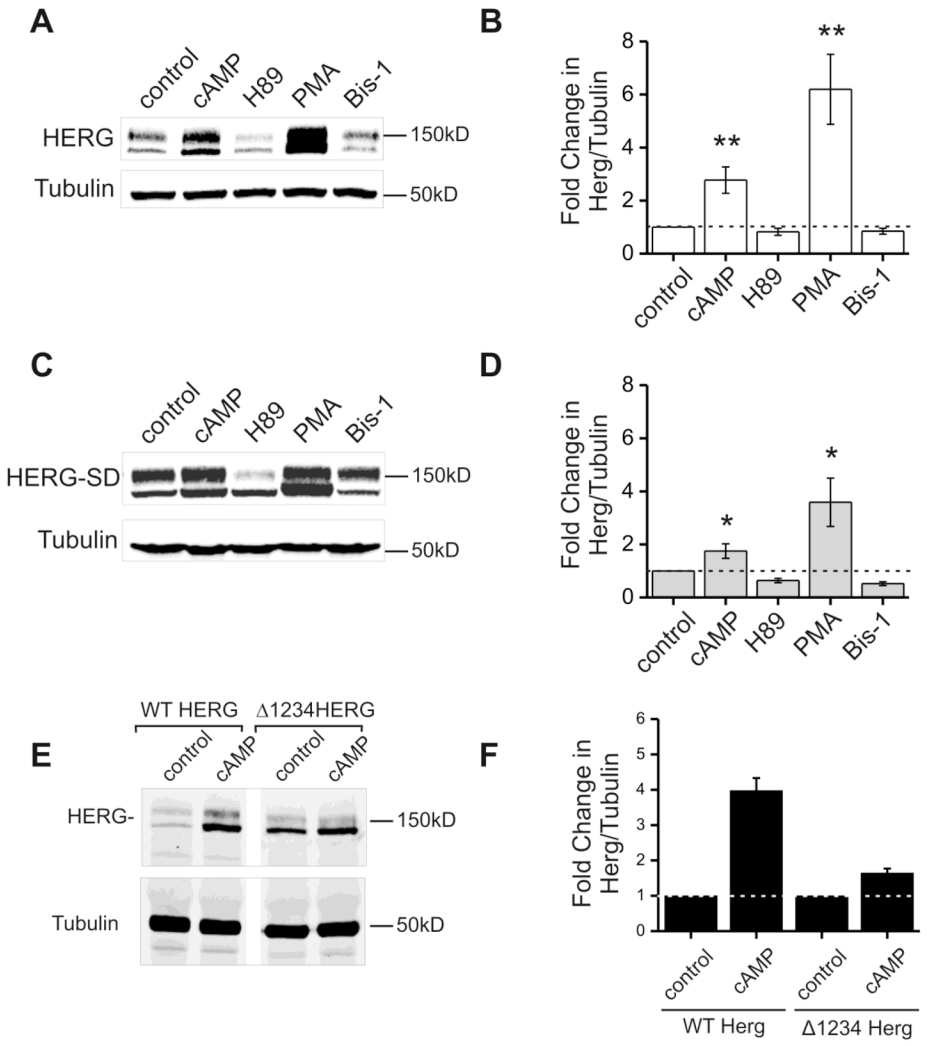

Figure 1. Kinase stimulation and inhibition modulate protein abundance of HERG-WT and HERG-SD

Parts A and C are representative immunoblots from HEK-HERG wild type and HEK-HERG-SD phosphomimetic mutant stably transfected cells after 24 hour treatment with control (DMSO), CPT-cAMP, H89, PMA, and bisindolylmaleimide-1 (bis-1). HERG appears as a doublet at 135 and 155 kD and tubulin was used as the loading control. Parts B and D show quantification and summary data for the experiment. In part B, cAMP and PMA treatment cause a three- and sixfold increase in wild type HERG protein abundance when normalized to tubulin. H89 and Bis-1 show slight decreases in HERG abundance. Part D shows that HERG-SD the phosphomimetic mutant increases in protein abundance upon both PKA and PKC activation. CPT-cAMP treatment results in a two-fold increase in HERG-SD while PMA causes a four-fold increase. Drug treatment samples were compared to the control, n=5 and * p-value < 0.05, ** p-value < 0.01. Part E is an immunoblot showing lysate from stably expressing HEK-HERG Δ1234 after treatment with control DMSO or CPT-cAMP. Lanes 1 and 2 show blots from cells expressing WT HERG and lanes 3 and 4 show from cells expressing Δ1234HERG. Tubulin was used as the loading control. Part F shows quantification of the fold change in WT HERG and Δ1234 HERG protein abundance normalized to tubulin where the DMSO controls were normalized to 1 (n=2).

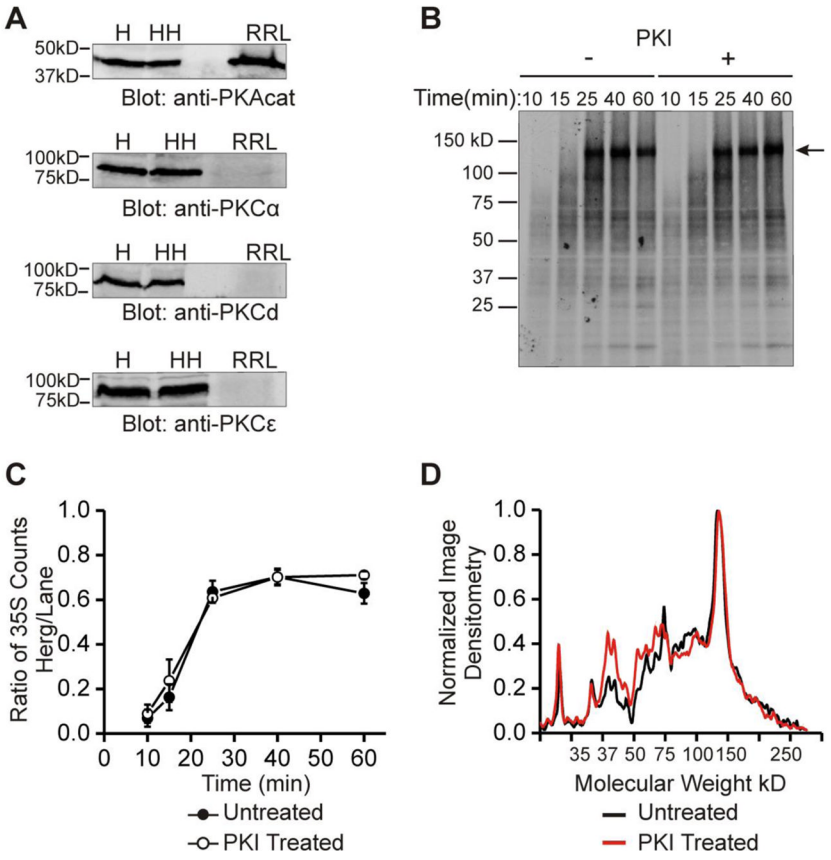

Figure 2. In vitro translation reveals that a cellular co-factor is necessary for changes in HERG protein abundance

Part A shows immunoblots of PKA and PKC isoforms. Top blot shows PKA catalytic subunit is present in H = HEK293 lysate, HH = HEK-HERG lysate, and RRL = rabbit reticulocyte IVT lysate. Bottom three blots show PKC isoforms α, δ, and ε are present in HEK293 and HEK-HERG lysate but absent in rabbit reticulocyte lysate. Part B shows an ^{35}S autoradiograph of labeled in-vitro translation products of HERG at five time points from 10 to 60 minutes and under the control condition (left half) or with addition of 10 μM PKI (right half). Arrow indicates full length HERG translation product at ~130 kD. Part C shows quantification and summary data of in-vitro translation experiments. The points graphed represent the ratio of ^{35}S counts of the full length product over that of the total lane at each time point. The points of the control experiment and the experiment with PKI addition are not statistically different, n=3. Part D shows a line scan plot where normalized image densitometry of the ^{35}S autoradiograph is plotted against increasing molecular weight. This analysis was done at 60 minutes of translation. Black line represents the control condition while red line represents the PKI treated condition. All plots were normalized to the value of the highest peak representing the full length HERG product and to zero for the baseline.

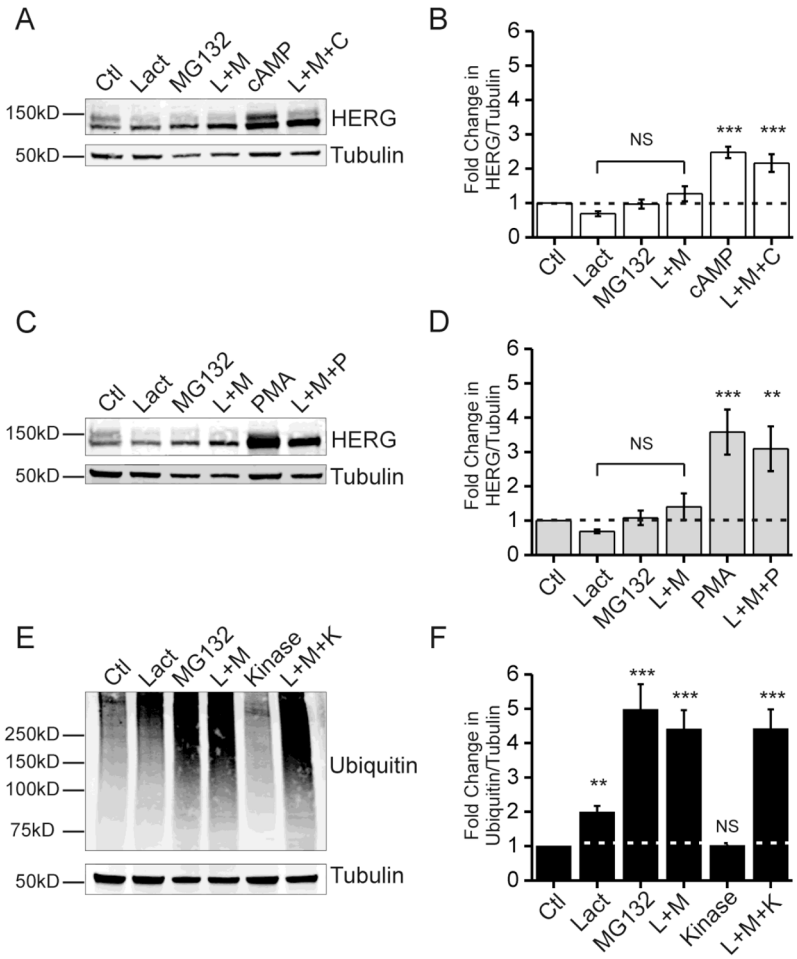

Figure 3. Proteasome inhibition does not mimic kinase stimulation

Parts A, C, and E show immunoblots from HEK-HERG stable cells treated with proteasome inhibitors and kinase stimulators. Part A shows a Western blot with the effect of proteasome inhibitor treatments with lactacystin (Lact), MG132, and combination treatment (L+M) to CPT-cAMP treatment (cAMP) and a combination of proteasome inhibitors plus CPT-cAMP (L+M+C). HERG appears as a doublet and tubulin was used as a loading control. Part B shows quantification and summary data for part A. Fold change in the ratio of total HERG over tubulin is plotted per treatment condition. Control levels are normalized to 1.0 as indicated by dotted line. The differences between control and proteasome inhibition samples were not statistically significant. The differences between control samples and cAMP treated samples were statistically significant, n=5 *** p-value <0.001. Part C shows Western blots from HEK-HERG stable cells treated with proteasome inhibitors and PMA. Part D shows quantification and summary data for part C. Fold-change in the ratio of HERG over tubulin is plotted for each treatment condition. The differences between control and proteasome inhibition samples were not statistically significant. The differences between control samples and PMA treated samples were statistically significant, n=5 ** p-value <0.01 and *** p-value <0.001. Part E shows Western blots for total ubiquitin under control, proteasome inhibition, kinase stimulation, and combination treatments. Ubiquitin appears as a smear and tubulin was used as a loading control. Part F shows quantification and summary data for part E. Fold change in the ratio of ubiquitin over tubulin is plotted per treatment condition. Control levels were normalized to 1.0 as indicated by dotted line. The difference between control and kinase treated samples was not significant. The differences between

control and proteasome inhibition samples were statistically significant, n=10 ** p-value <0.01 and *** p-value < 0.001.

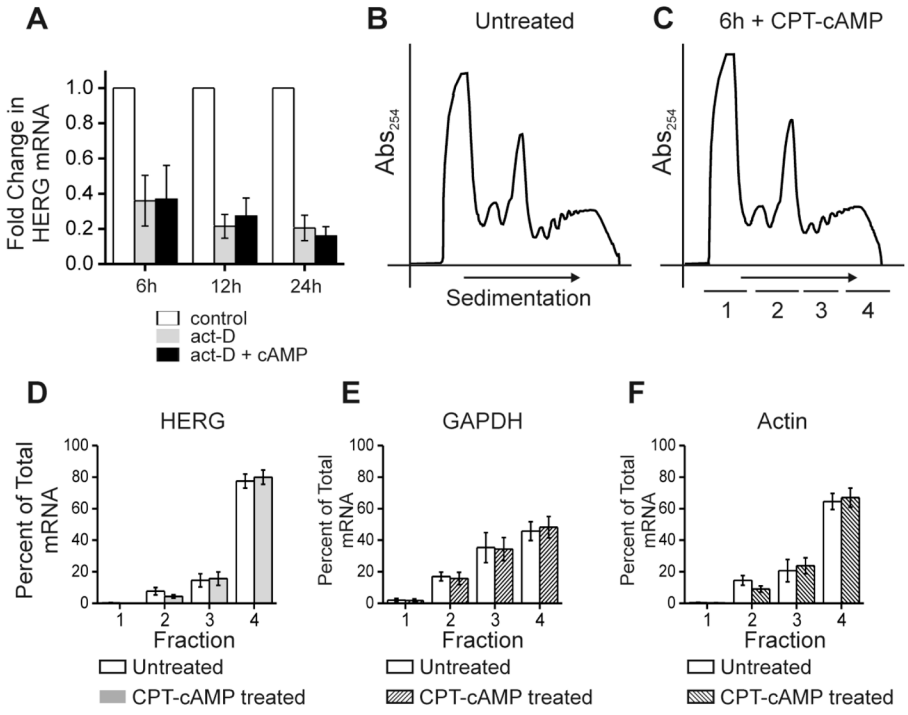

Figure 4. cAMP treatment does not alter HERG mRNA stability nor alter the association with polysomes

Part A shows quantification of HERG mRNA levels (normalized to GAPDH mRNA levels) by quantitative real-time PCR for an experiment testing the stability of HERG mRNA after treatment with actinomycin-D alone (act-D) or in combination with CPT-cAMP (act-D +cAMP) over a time course. HERG mRNA levels were compared between the control condition (DMSO treated) and act-D or act-D + cAMP treatments at each of the three time points 6, 12 and 24 hours. Control sample fold change was normalized to 1.0, act-D treatment is shown in gray and act-D + cAMP treatment is shown in black. The differences between act-D and act-D + cAMP treatments were not statistically significant at any time point, n=3. Parts B and C show a separate experiment, they are polyribosomal profiles for untreated and 6-hour CPT-cAMP treated conditions. The y-axis shows absorbance at 254 nm plotted against increasing gradient density where heaviest components will sediment to the right. The underlined segments 1–4 show where fractions were collected for subsequent qRT-PCR. Parts D-F show summary data for results of qRT-PCR. The y-axis values represent percent of total RNA that is comprised by (D) HERG, (E) GAPDH, and (F) Actin, respectively per fraction. Open bars show the untreated condition while shaded bars show the cAMP treated condition. Differences between treated and untreated conditions were not significant, n=4.

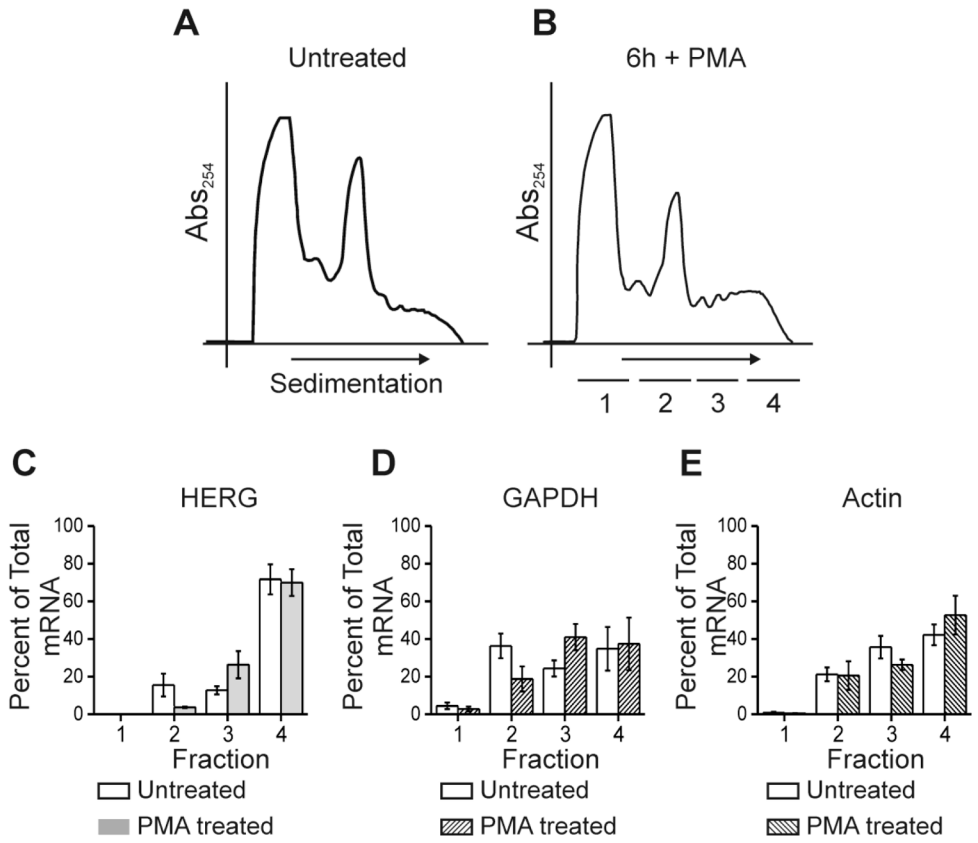

Figure 5. PMA treatment does not alter HERG mRNA association with polysomes

Parts A and B show polyribosomal profiles for untreated and 6-hour PMA treated conditions. The y-axis shows absorbance at 254 nm plotted against increasing gradient density where heaviest components will sediment to the right. The underlined segments 1–4 show where fractions were collected for subsequent qRT-PCR. Parts C-E show summary data for results of qRT-PCR. The y-axis values represent percent of total RNA that is comprised by (C) HERG, (D) GAPDH, and (E) Actin, respectively per fraction. Open bars show the untreated condition while shaded bars show the cAMP treated condition. Differences between treated and untreated conditions were not significant, n=4.

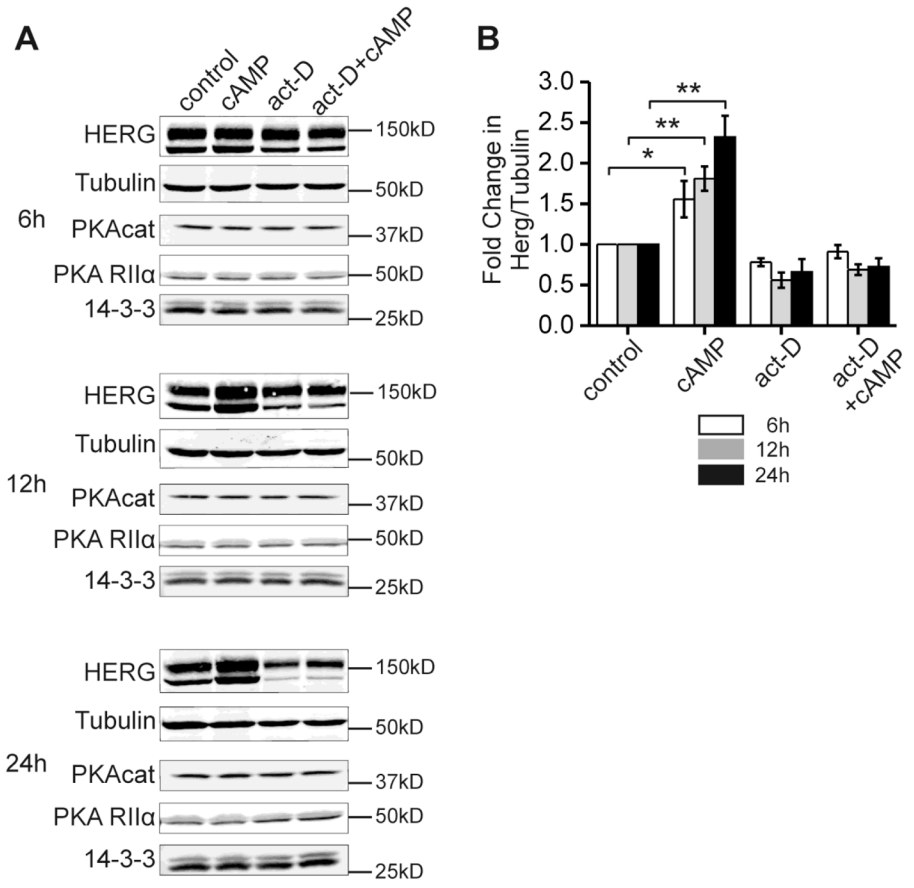

Figure 6. Transcriptional inhibition abolishes the cAMP-induced increase in HERG abundance

Part A, a series of immunoblots from HEK-HERG stable cells of HERG and tubulin under control (DMSO), CPT-cAMP treated, actinomycin-D treated, and combination cAMP and actinomycin-D treatment at three time points 6, 12, and 24 hours. HERG appears as a doublet and tubulin was used as the loading control. Lower panels show blots of PKA catalytic subunit-α, PKA regulatory subunit RIIα and multiple isoforms of 14-3-3. Part B shows quantification and summary data for the experiment. Fold change in the ratio of HERG protein over tubulin is plotted per treatment condition for each of the three time points. Control levels are normalized to 1.0 for all time points. Differences between the control and CPT-cAMP treated conditions are significant as indicated, n=5 and * p-value < 0.05, ** p-value < 0.01. Differences between the control and act-D conditions were not statistically significant. Differences between the control and combination treatment conditions were also not statistically significant. There were no significant changes with treatments compared to control for the levels of PKAcat, PKA RIIα and 14-3-3.

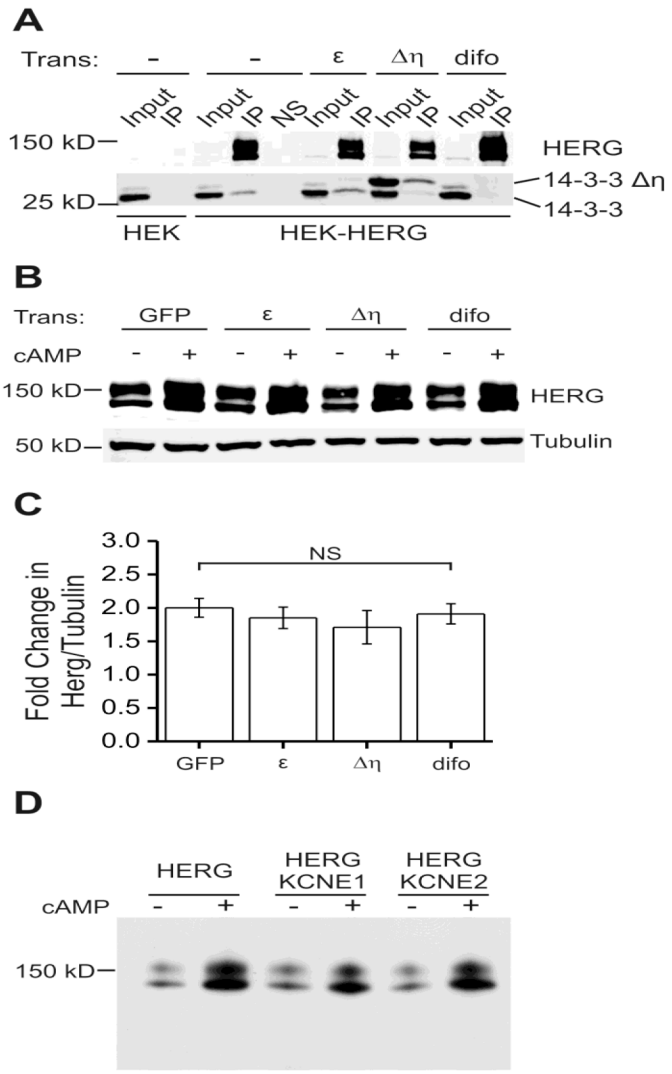

Figure 7. 14-3-3 and KCNE protein binding do not affect the cAMP-induced increase in HERG abundance

Part A shows immuno-precipitations (IP) from blank HEK or stably expressing HEK-HERG cells with additional transient transfection. Transient transfections were with 14-3-3ε, 14-3-3Δη (dominant negative mutant), and difopein (peptide blocker). The first two lanes of the top panel show a negative control, immunoprecipitation in HEK cells that do not express HERG. Top panel shows input lanes and IP lanes, where HERG is enriched in the IP, and another negative control NS which is mock immunoprecipitation with non-specific IgG. Lower panel shows 14-3-3 isoforms as two distinct bands which co-immunoprecipitated with HERG. The dominant negative mutant 14-3-3Δη migrates at a higher molecular weight. Transient transfection with 14-3-3Δη decreased the amount of endogenous 14-3-3 (lower band) that co-immunoprecipitated with HERG. Transient transfection with difopein abolished the HERG and 14-3-3 binding and thus 14-3-3 is absent in that lane. Part B shows an immunoblot of stably expressing HEK-HERG cells with various transient transfections and 24 hour CPT-cAMP treatment. Transient transfections are with GFP, 14-3-3ε, 14-3-3Δη, and difopein. Upper panel shows HERG protein abundance increases with CPT-cAMP treatment under all transfection conditions. The lower panel shows tubulin as the loading control. Part C shows quantification and summary data for the experiment in part B.

The fold changes in HERG normalized to tubulin are similar for all the transient transfection conditions. The differences between GFP transfected and 14-3-3ε, 14-3-3Δη, or difopein transfected groups are not significant, n= 8–27. Panel D shows immunoblots of HEK_HERG cells transiently transfected with GFP (HERG), mink (KCNE1) or MiRP1 (KCNE2) at baseline and after 24-hour stimulation with CPT-cAMP. The cAMP-dependent induction of HERG was not significantly altered by the co-expression of the KCNE family of interacting proteins.

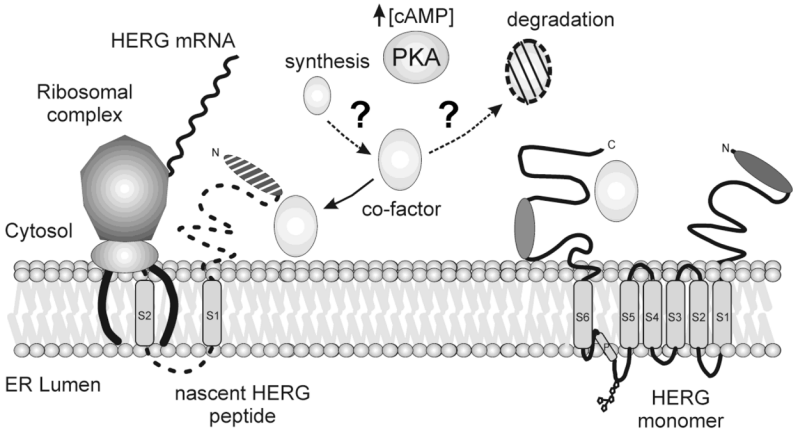

Figure 8. Model of HERG translation and key mediators

A schematic representation of HERG synthesis at the ER and key mediators that regulate the process. The fully synthesized HERG monomer is shown at right on the ER membrane with cytosolic N and C-termini and six transmembrane domains. At left is shown a simplified view of the ribosomal complex as it translates HERG mRNA into protein. The large and small subunits join with the translocon complex to synthesize the nascent HERG peptide. PKA and increased levels of cAMP may be responsible for mediating synthesis or turnover of an unknown co-factor. Several possibilities exist for the role of the co-factor and may play a part in aiding or accelerating HERG synthesis.